Journal Pre-proof

Progression of Parenchymal and Ductal Findings in Patients with Chronic Pancreatitis: A 4-Year Follow-Up MRI Study

Emilie Steinkohl, Søren Schou Olesen, Esben Bolvig Mark, Tine Maria Hansen, Louise Kuhlmann Frandsen, Asbjørn Mohr Drewes, Jens Brøndum Frøkjær

PII: S0720-048X(20)30057-7

DOI: https://doi.org/10.1016/j.ejrad.2020.108868

Reference: EURR 108868

To appear in: *European Journal of Radiology*

Received Date: 3 December 2019

Revised Date: 23 January 2020

Accepted Date: 4 February 2020

Please cite this article as: Steinkohl E, Schou Olesen S, Bolvig Mark E, Hansen TM, Kuhlmann Frandsen L, Mohr Drewes A, Brøndum Frøkjær J, Progression of Parenchymal and Ductal Findings in Patients with Chronic Pancreatitis: A 4-Year Follow-Up MRI Study, *European Journal of Radiology* (2020), doi: https://doi.org/10.1016/j.ejrad.2020.108868

Progression of Parenchymal and Ductal Findings in Patients with Chronic Pancreatitis: A 4-Year Follow-Up MRI Study

Emilie Steinkohl[a,b], Søren Schou Olesen[b,c], Esben Bolvig Mark[a,c], Tine Maria Hansen[a,b], Louise Kuhlmann Frandsen[b,c], Asbjørn Mohr Drewes[b,c], Jens Brøndum Frøkjær[a,b]

a) Mech-Sense, Department of Radiology, Aalborg University Hospital, Hobrovej 18-22, 9000 Aalborg, Denmark.

b) Department of Clinical Medicine, Aalborg University, Søndre Skovvej 11, 9000 Aalborg, Denmark.

c) Centre for Pancreatic Diseases, Department of Gastroenterology & Hepatology, Aalborg University Hospital, Mølleparkvej 4, 9000 Aalborg, Denmark.

Short title: Progression of imaging features in chronic pancreatitis

Word count: Abstract: 246; Main text: 3600; References: 38; Figures 3; Tables: 4.

Correspondence:

Professor Jens Brøndum Frøkjær, MD, PhD

Department of Radiology

Aalborg University Hospital

P.O. Box 365

DK-9100 Aalborg, Denmark

Telephone: +45 9766 5105; Fax number: +45 9766 5257

E-mail: jebf@rn.dk

Highlights:

Morphological progression in chronic pancreatitis seems to be parenchymal-related

The different morphological changes in the pancreas were unrelated

Parenchymal MRI-parameters represent sensitive biomarkers for disease progression

Ductal-related MRI-parameters are not sensitive biomarkers for disease progression

Abstract

Purpose: Knowledge of the underlying mechanisms behind progression of chronic pancreatitis (CP) is needed to identify targets for new mechanism-based treatments. There is an urgent need for imaging biomarkers that can detect early morphological and functional pancreatic damage in order to initiate intervention and reduce the progression of CP at an early stage. The aim of our study was to assess and explore the potential role of structural magnetic resonance imaging (MRI) biomarkers for characterisation of disease progression in a CP patient cohort over a 4-year period.

Methods: This longitudinal MRI study included twenty-five patients with definitive CP. Assessments of morphological imaging parameters at baseline and after 4 years included pancreatic gland volume, apparent diffusion coefficient (ADC) values, fat signal fraction (FSF) and main pancreatic duct (MPD) diameter. Patients were classified according to the modified Cambridge classification.

Results: CP patients developed significantly reduced pancreatic gland volume, which decreased from mean 50.3±19.6 ml at baseline to 43.5±20.8 ml at follow-up (P<0.001), decreased ADC values, meaning a higher degree of fibrosis (P<0.001), increased FSF, meaning more fat infiltration (P<0.001) and higher Cambridge classification scores (P=0.033). The MPD diameter in the pancreatic head, body and tail did not change significantly over time (all P>0.05). Only few, but no clear and systematic, associations were found between the progressions of the individual MRI measures.

Conclusions: Morphological progression in patients with established CP seems to be primarily parenchymal-related. The different parenchymal changes were mostly unrelated and probably reflect diverse pathophysiological processes.

Abbreviations: CP: chronic pancreatitis; MRI: magnetic resonance imaging; MPD: main pancreatic duct; ADC: apparent diffusion coefficient; FSF: fat signal fraction; ERCP: endoscopic retrograde cholangiopancreatography; DWI: diffusion-weighted imaging; AP, anterior-posterior; ROI: region of interest

Key words: Chronic Pancreatitis; Magnetic Resonance Imaging; Fibrosis; Atrophy

Introduction

Chronic pancreatitis (CP) is a progressive fibro-inflammatory disease, associated with considerable morbidity and a fivefold increased mortality compared to the background population [1]. The incidence of CP is rising and has been estimated to approximately 100 per 100.000 inhabitants per

year in the Western world [2]. CP is characterised by irreversible functional and morphological changes of the pancreatic gland, which can cause pancreatic duct deformation and strictures, pancreatic atrophy and fibrosis, chronic visceral pain and impairment of exocrine and endocrine functions [3].

Since no effective treatment of established CP exists, there has been an increased focus on early detection and intervention [4]. Still, the mechanisms behind the development and progression of CP are incompletely understood. The need for establishing non-invasive biomarkers (including imaging) as a surrogate for clinical disease progression has been highlighted recently. Hence, detection of early morphological and functional pancreatic damage may facilitate mechanism-based therapy and interventions and reduce the progression of CP at an early stage [5,6]. Also, such biomarkers might be suited to identify mechanism-based targets for therapy. However, to establish such meaningful imaging parameters in monitoring and predicting disease progression, testing and validation in longitudinal studies are needed.

The Cambridge classification has been used since 1984 as a reference standard in diagnosing and staging CP by endoscopic retrograde cholangiopancreatography (ERCP) [7]. However, ERCP is an invasive procedure that carries risk of severe complications, including post-ERCP pancreatitis. Moreover, ERCP does not allow evaluation of the pancreatic parenchyma. Therefore, ERCP is now rarely used as a diagnostic tool. The morphological changes of pancreas in CP can be detected by computed tomography, magnetic resonance imaging (MRI), and ultrasound (transabdominal and endoscopic) [7,8]. In recent years, technical developments in MRI allow a comprehensive assessment of the complex morphological parenchymal- and ductal-related changes associated with CP. Besides conventional T1- and T2-weighted imaging that conveys information on pancreatic anatomy and atrophy, diffusion-weighted imaging (DWI) is valid for the assessment of pancreatic fibrosis [9–11]. Additionally, Dixon imaging with the assessment of fat signal fraction (FSF), is a promising marker

of pancreatic fat content [12]. Altogether, these MRI techniques might serve as quantitative non-invasive imaging biomarkers reflecting the different stages in the progression of CP [13]. So far, no longitudinal studies have explored the role of quantitative MRI for characterisation of morphological progression in CP.

The primary objective of this longitudinal study was to assess and explore the potential role of structural quantitative MRI biomarkers for characterisation of disease progression in a well-characterised CP patient cohort over 4 years. We aimed to (1) characterise progression in parenchymal-related MRI parameters, including pancreatic atrophy, fibrosis, fat infiltration, and ductal-related parameters, and (2) to explore the associations between the progressions of different MRI assessment parameters.

2. Materials and methods

2.1. Participants and study design

This was a 4-year prospective study conducted at Centre for Pancreatic Diseases, Departments of Gastroenterology and Radiology, Aalborg University Hospital, Denmark. Patients underwent MRI examination at: (1) a baseline visit (December 2013 to January 2015) and (2) a follow-up visit (September to December 2018). Patients were recruited at baseline from our outpatient clinic and baseline data were originally used for a cross-sectional study assessing pancreatic MRI in patients with CP [12]. Enrolment of patients is described in Fig. 1.

Initially, MRI was performed in 82 patients diagnosed with CP. The diagnosis was based on the Lüneburg criteria [8]. Inclusion criteria were pancreatic gland volume more than 20 ml assessed at the baseline study [12] to allow a valid assessment of parenchymal MRI features. Exclusion criteria were: (1) inability to undergo MRI, (2) major illness such as cancer, and (3) major pancreatic surgery. Among the 82 patients initially included, 34 patients did not fulfil these criteria, and thus 48 patients were eligible for the follow-up study. Of these 48 patients, 25 were available for re-scanning.

The North Denmark Region Committee on Health Research Ethics (N-20130040; N-20130059) approved the study and all patients provided oral and written informed consent. The study was conducted in accordance with the Declaration of Helsinki.

2.2. Magnetic resonance imaging

MRI was performed on all patients in the same 1.5T MR scanner (Signa HDxt, General Electric Healthcare, Milwaukee, Wisconsin, USA) using an 8-channel body coil, supine position. The imaging protocol included exactly the same sequences at the baseline and follow-up scan: (1) T2-weighted

balanced steady-state gradient echo acquisition (FIESTA, axial, slice thickness 4 mm), (2) T2-weighted single-shot fast spin echo (SSFSE, fat saturated, axial, slice thickness 5 mm), (3) 3-dimensional magnetic resonance cholangiopancreatography (MRCP, coronal, free breathing, slice thickness 2.6 mm), (4) T2-weighted single-shot respiratory triggered (T2 SS RTr, coronal, slice thickness 2.5 mm), (5) diffusion weighted imaging (DWI, axial, TR/ TE 4000/70 ms, slice thickness 6 mm) with b-values 50, 400 and 800 s/mm^2, and (6) 3-dimensional rapid gradient echo sequences (LAVA-flex, axial, slice thickness 2.6 mm) generating in-phase and out-of-phase images and afterwards, by applying two-point Dixon technique, reconstruction of fat-only and water-only images. A radiologist in training (ES) under guidance and review by a senior radiologist (JBF), with 17 years of experience, performed the MRI evaluations and measurements.

2.3. Assessment of gland volume and anterior-posterior diameters

For assessment of parenchymal thickness, the anterior-posterior (AP) diameter was measured at standardised positions in the pancreatic head, body and tail [13], see Fig. 2. The pancreatic gland volume measurements were generated on T2-weighted FIESTA images in a customised application implemented in Matlab 2013b (MathWorks, Natick, Massachusetts USA), as described previously [12]. Contour of the pancreas was segmented on each slice and the gland volume was automatically calculated by adding the areas in all slices and multiplying them by slice thickness, excluding main pancreatic duct segments and cystic lesions.

2.4. Assessment of pancreatic diffusion and fat content

All regions of interest (ROIs) for diffusion and fat content assessments were the same size and placed in the same position within each subject. The ROIs for each region in the pancreatic head, body and tail covered a circular area between 40 and 100 mm^2 (mean 62.3 mm^2). The anatomical boundaries

of the pancreatic regions were determined as follows: the head was defined as the portion to the left border of the superior mesenteric vein; the portion of pancreas between the left border of the superior mesenteric vein and the left border of aorta were bisected into the body (the right half) and the tail (the left half) [14,15]. All ROIs were placed in these anatomical regions and carefully positioned away from the pancreatic border in order not to falsely include extra-pancreatic tissue and prevent volume-averaging effects. In addition, effort was made to avoid cystic lesions, vessels and ducts, by using other image series such as the T2-weighted as anatomical map.

2.5. Measurement of pancreatic diffusion

Pancreatic apparent diffusion coefficient (ADC) maps were generated by a commercially available software (AW server 2.0, General Electric, Milwaukee, Wisconsin, USA) from the DWI series. Pancreatic ADC values were automatically calculated by drawing ROIs in the pancreatic head, body and tail on the corresponding ADC maps.

2.6. Measurement of pancreatic fat signal fraction

The analysis of FSF was performed on the fat-only and water-only images of the LAVA-flex (Dixon) sequence using the commercially available software EazyViz (v. 7.6.7-270, Karos Health A/ S, Valby, Denmark). ROIs were placed in the pancreatic head, body and tail. The mean signal intensity (SI) in the ROIs was used to calculate FSF by using the formula: $SI_{fat\text{-}only} / (SI_{water\text{-}only} + SI_{fat\text{-}only})$.

2.7. Assessment of ductal changes

The maximal AP diameter of the MPD, pathological side branches, pseudocysts with a diameter more than 5 mm, the presence of ductal obstruction, as well as the presence of intraductal filling defects

were assessed, in accordance with the international imaging guidelines for CP [13], on 3-dimensional MRCP and T2-weighted images using EazyViz. This information and other parenchymal features were used to characterise all CP patients according to the modified Cambridge classification used for CT/MRCP [16,17]. Due to the small number of patients in some Cambridge classification subgroups, patients were merged into two groups (Cambridge I-II and Cambridge III-IV) to compare the development in Cambridge classification scores.

2.8. Assessment of clinical parameters

In addition to MRI, the following clinical parameters were obtained in all patients on both visits: (1) aetiology of CP, (2) duration of CP, from the initial diagnosis until the baseline MRI scan, (3) presence of diabetes, (4) presence of exocrine insufficiency (defined as faecal elastase <200µg/g[18]) and (5) body mass index (kg/m^2).

2.9. Statistics

The data are expressed as mean ± SD for continuous variables and numbers (percentages) for categorical variables unless otherwise indicated. The assumption of normality was checked by inspection of Q-Q plots and skewness/kurtosis tests for normality. If the variables were normally distributed, dependent t-test was performed for continuous variables and McNemar's test was performed for categorical variables. If the assumption of normality was not met, two-sample Wilcoxon rank-sum (Mann-Whitney) test was used. Pearson correlation was used for analysing the associations between the different MRI parameters. Spearman's test was used for non-parametric analysis. A P-value less than 0.05 was considered statistically significant. The software package STATA version 15.2 (StataCorp LP, College Station, Texas, USA) was used.

3. Results

3.1. Demographic and clinical characteristics

The demographic and clinical characteristics of the enrolled patients are reported in Table 1.

3.2. Progression of morphological imaging parameters

The MRI based imaging parameters assessed at baseline and follow-up are presented in Table 2. Fig. 2 illustrates imaging findings in a representative patient at baseline and follow-up. The mean time interval between the two MRI examinations was 4.3±0.3 years. Compared with the baseline scan, patients developed reduced parenchymal thickness at follow-up in the pancreatic head, body and tail (all $P<0.001$), and a higher degree of pancreas atrophy, i.e. reduction in volume ($P<0.001$, Table 2 and Fig. 3). Also, patients developed lower ADC values, indicating an increased degree of fibrosis, in the pancreatic head ($P<0.001$), body ($P<0.001$) and tail ($P=0.002$) during the follow-up period, see Fig. 3. The FSF (indicating the degree of fat infiltration) increased in the pancreatic head ($P=0.001$), body ($P=0.001$) and tail ($P=0.024$) during the follow-up period, see Fig. 3.

The Cambridge classification scores were higher at follow-up compared to baseline ($P=0.033$), see Table 2. The maximal overall MPD diameter showed great variation in size during the disease course, and was 5.5 mm (range: 2–15 mm) at the baseline and 6.7 mm (2–18 mm) at follow-up, but the 4-year change in MPD diameter was not significant ($P=0.23$). Also, changes in the remaining ductal related parameters did not change significantly over time (all $P>0.05$).

3.3. Associations between morphological imaging parameters at baseline

Associations between fibrosis, fat infiltration and ductal pathology at baseline are shown in Table 3.

For the atrophy-related parameters, pancreatic gland volume correlated positively with parenchymal thickness of the pancreatic head (r=0.7, P<0.001), body (r=0.46, P=0.020) and tail (r=0.43, P=0.033). At baseline, the degree of pancreatic atrophy was not associated with the degree of pancreatic fibrosis, fat infiltration or the ductal related parameters (all P>0.05). There was a positive correlation between the ADC of the pancreatic head and the Cambridge classification scores (r=0.49, P=0.015). The pancreatic fat content (FSF) was not associated with any of the other morphological parameters. For the ductal related parameters the maximal MPD diameter of the pancreatic body was associated with the Cambridge classification (r=0.52, P=0.008). There were no associations between the atrophy- and ductal-related parameters (all P >0.05).

3.4. Associations between progressions in morphological imaging parameters

Associations between the 4-year changes in the various MRI assessment parameters are reported in Table 4. For the atrophy-related parameters, the change in pancreatic gland volume correlated positively with the changes in parenchymal thickness of the pancreatic head (r=0.7, P<0.001), body (r=0.64, P<0.001) and tail (r=0.55, P=0.005). The progression in pancreatic atrophy was not associated with the progression of Cambridge classification/MPD diameter or degree of progression in pancreatic fibrosis (all P>0.05). For the fat infiltration, the changes in FSF, i.e. ΔFSF of the pancreatic head, was positively correlated with the changes in the Cambridge classification (r=0.49, P=0.016). For the ductal related parameters, the progression in Cambridge classification correlated positively with changes in MPD of the pancreatic tail (r=0.67, P=<0.001) and negatively with changes in ADC, i.e. ΔADC tail (r=-0.61, P=0.005). None of the remaining MRI parameters of the pancreas were associated with neither parenchymal nor the ductal-related parameters, see Table 3.

4. Discussion

To our best knowledge, this study is the first to explore the role of quantitative MRI for characterisation of morphological progression in a cohort of CP patients. The baseline MRI examination confirmed findings from previous studies [10,12], which demonstrated that patients with established CP have a high degree of atrophy, fibrosis and fat infiltration as well as ductal changes of the MPD. After 4 years, patients showed a significant and pronounced progression in the parenchymal related morphological parameters; however, the changes in ductal pathology showed a wide variation in size without significant progression for most parameters. Only Cambridge classification scores worsened over time, but findings were less pronounced as compared with those of the parenchyma. Interestingly, there were only few, but no clear and systematic, associations between the progression in different quantitative parenchymal and ductal-related MRI parameters, which emphasises the fact that different pathophysiological processes are likely involved in CP progression. Our data suggest that parenchymal parameters, including pancreatic volume as well as degree of fibrosis and fat infiltration, represent more sensitive biomarkers for disease progression, compared to the currently used ductal-based staging system (Cambridge classification).

The parenchymal changes in CP comprise of both shrinkage of the pancreatic gland and replacement of glandular elements by fat and fibrotic tissue. This can result both in development of pancreatic endocrine and exocrine insufficiency as well as chronic abdominal pain. In our study, all patients showed an increased degree of atrophy with lower volumes than in the normal pancreas [12,19]. The degree of atrophy might be a well-suited parameter for monitoring of the morphological progression of CP. An abdominal MRI animal study by Szczepaniak et al. showed that abdominal MRI allows accurate and reproducible evaluation of pancreatic volume, with a strong correlation with the post-mortem volume assessment [20]. Moreover, our study is in line with a recent study by Kipp

et al. showing a strong correlation between the pancreatic gland volume and the AP diameter of the pancreatic head, body and tail [21]. This implies that instead of the laborious measurement of the pancreatic volume, the much simpler and faster measurement of the pancreatic AP diameters may also be useful to assess the degree of atrophy in an easy, precise and accurate way for clinical use. Even though there were no healthy controls enrolled in our study, the rate of volume loss of the pancreatic gland was indeed higher than the age-related volume loss of the healthy population, as shown by Kipp et al[21].

Several studies have found reduced pancreatic water diffusion (lower ADC values) in patients with CP compared to the normal pancreas, and interestingly the ADC values were related to the degree of fibrosis assessed histologically [9,15,22]. At baseline, patients had reduced ADC values and further reduction was observed during the follow-up period. This finding attest to the understanding of CP as a progressively evolving fibro-inflammatory disease, where the pancreatic parenchyma is gradually replaced by fibrotic tissue. The relevance of fibrosis progression in CP development is further supported by recent studies proposing stimulation and conversion of pancreatic stellate cells into myofibroblasts, which are responsible for the collagen production and the formation of parenchymal fibrosis [23–25]. This results in permanent loss of the normal pancreatic parenchyma and structure, as well as deformation of the ductal system, etc. [26]. Our findings, showing primarily parenchymal progression with atrophy, fibrosis and fat infiltration, are in line with these assumptions, as they identify the increase of fibrogenesis to be an important factor in the disease development. Hence, the changes in degree of pancreatic fibrosis may serve as a useful imaging biomarker reflecting the different stages of progression in CP patients.

At baseline patients had a high degree of fat infiltration [12], and a further increase of the pancreatic fat content was observed during the 4-year period. A study by Schrader et al. showed that the fibrosis in CP was often accompanied by large areas of adipose tissue, a feature that was not found

in the healthy pancreas [27]. We could confirm this in our study, as the patients showed both increased content of pancreatic fat and degree of fibrosis (as measured with ADC). Furthermore, a previous study by Yoon et al. has shown that pancreatic fat fractions showed a moderate correlation with the histological fat content [28,29]. Altogether, the pancreatic FSF is considered as a good non-invasive proxy of the histological fat content. Moreover, the assessment of fat infiltration using MRI is reported superior to other techniques, like ultrasonography, computed tomography or dual-echo chemical shift imaging [30,31]. The progression of pancreatic fat infiltration might support that different stages of in progression of CP may be defined.

A striking finding of our study is that the degree of progression in MPD diameter did not change significantly during the 4-year period and only moderate changes in the proportionate distributions of the modified Cambridge classification score subgroups were observed. This implies that ductal progression may be an insensitive biomarker of CP progression once the disease is established. In addition, the MPD diameter showed a pronounced variation between and within patients, which may be explained by dynamic processes in the ductal system such as calibre variations due to strictures that are likely to change over time. This is an interesting finding as most of the established CP imaging grading systems traditionally are based on ductal changes, originally developed for CP classification based on ERCP. This means that especially ductal changes laid the foundation for the established diagnosis and staging systems of the disease; however, our findings indicate that these traditional staging systems should likely be revised. Further, a recent study has shown that the ductal-related parameters such as dilated side-ducts, ductal irregularity and calibre variation has a low inter-reader agreement [32]. Altogether, assessments of the ductal system may not be an ideal imaging biomarker for monitoring of disease progression in the context of CP.

The changes in MRI assessment parameters reflecting pancreatic fibrosis, the degree of pancreatic fat infiltration and the degree of the atrophy-related parameters were not associated. Moreover, there

was only weak associations between 4-year progression in ductal-related parameters and parenchymal related MRI parameters. This indicates that the different structural pancreatic changes (parenchymal- and ductal-related) in patients with CP seem to be complex, independent and probably driven by partly unrelated pathophysiological processes. These different pathophysiological processes may potentially depend on different risk factor for CP, i.e. toxic exposure (alcohol and tobacco consumption), genetic factors, different aetiologies or anatomical differences and may for that reason be potential biomarkers of prognostication of the disease course in different subgroups of CP patients. Future prospective MRI studies should explore this further.

The presented MRI assessment parameters may be useful as non-invasive imaging biomarkers reflecting the different stages of fibrosis, fat infiltration and atrophy in the progression of CP. This could support therapeutic decision-making and monitoring of anti-fibrotic therapies in the future. As the progression of disease in patients with established CP seems to be primarily parenchymal-related, it will also be important to identify new methods to detect the minor structural damage of the parenchyma useful for diagnosing CP in earlier stages. DWI has shown a respectable diagnostic accuracy in stratifying advanced fibrosis [9], but in the recent years there has been a tremendous technical development in MRI techniques providing even more detailed information on pancreatic fibrosis by using novel MRI techniques, such as T1-mapping, intravoxel incoherent motion imaging (DWI with multiple b-values and assessment of diffusion and perfusion fractions) and MR elastography with assessment of tissue stiffness [33–38]. These techniques could potentially give even better biomarkers for the milder degrees of CP.

There are also a number of limitations in this study. First, our sample size was relatively small, and we had a considerable drop-out rate (48 %). The fact that 23 patients were not available for the re-scanning, may have contributed to the MRI results at the 4-year follow-up, as these patients could have shown other patterns of morphological progression in CP. Additionally, factors such as diabetes,

previous alcohol misuse, malnutrition, and other comorbidities could potentially have an impact on the MRI findings. Also, the lack of healthy controls in this study is a limitation. Future studies should include larger sample sizes and patients with milder degrees of disease as well as shorter disease duration, and also healthy control subjects, to better explore the full range of the pathophysiological mechanisms involved in the progression of CP.

One of the major strengths of this study is the longitudinal study design regardless of the very challenging patient group. Furthermore, it is a strength to gain MRI data from the same scanner using the same quantitative imaging protocol.

5. Conclusions

Patients showed a significant and pronounced progression in the parenchymal related morphological parameters between scans repeated after four years; whereas the changes in ductal pathology showed a wide variation in size with only the Cambridge classification score being significant. Progression of the different morphological changes of the pancreas (i.e. atrophy, fibrosis, fatty infiltration and ductal pathology) in patients with CP seemed to be independently unrelated and parallel processes, which could indicate a complex and independent pathogenesis behind development of CP. Inclusion of multiple quantitative MRI features of the pancreas will likely be needed to provide clear disease staging and to fully explore the mechanisms of disease progression in CP.

Acknowledgements

The authors thank radiographer Kenneth Krogh Jensen for his assistance in data collection.

REFERENCES

[1] U.C. Bang, T. Benfield, L. Hyldstrup, F. Bendtsen, J.E. Beck Jensen, Mortality, cancer, and comorbidities associated with chronic pancreatitis: A Danish nationwide matched-cohort study, Gastroenterology. 146 (2014) 989–994.e1. https://doi.org/10.1053/j.gastro.2013.12.033.

[2] D. Yadav, L. Timmons, J.T. Benson, R.A. Dierkhising, S.T. Chari, Incidence, prevalence, and survival of chronic pancreatitis: A population-based study, Am. J. Gastroenterol. 106 (2011) 2192–2199. https://doi.org/10.1038/ajg.2011.328.

[3] P.A. Jamidar, Chronic pancreatitis, a comprehensive review and update. Part I: Epidemiology, etiology, risk factors, genetics, pathophysiology, and clinical features, Disease-a-Month. 60 (2014) 530–550. https://doi.org/10.1016/J.DISAMONTH.2014.11.002.

[4] D.C. Whitcomb, Better Biomarkers for Pancreatic Diseases, Pancreas. 44 (2015) 1171–1173. https://doi.org/10.1097/mpa.0000000000000550.

[5] D.C. Whitcomb, D. Yadav, S. Adam, R.H. Hawes, R.E. Brand, M.A. Anderson, M.E. Money, P.A. Banks, M.D. Bishop, J. Baillie, S. Sherman, J. DiSario, F.R. Burton, T.B. Gardner, S.T. Amann, A. Gelrud, S.K. Lo, M.T. DeMeo, W.M. Steinberg, M.L. Kochman, B. Etemad, C.E. Forsmark, B. Elinoff, J.B. Greer, M. O'Connell, J. Lamb, M.M. Barmada, North American Pancreatic Study Group, Multicenter Approach to Recurrent Acute and Chronic Pancreatitis in the United States: The North American Pancreatitis Study 2 (NAPS2), Pancreatology. 8 (2008) 520. https://doi.org/10.1159/000152001.

[6] D.C. Whitcomb, L. Frulloni, P. Garg, J.B. Greer, A. Schneider, D. Yadav, T. Shimosegawa, Chronic pancreatitis: An international draft consensus proposal for a new mechanistic definition, Pancreatology. 16 (2016) 218–224. https://doi.org/10.1016/j.pan.2016.02.001.

[7] M. Sarner, P.B. Cotton, Classification of pancreatitis., Gut. 25 (1984) 756–759. https://doi.org/10.1136/GUT.25.7.756.

[8] P.G. Lankisch, N. Breuer, A. Bruns, B. Weber-Dany, A.B. Lowenfels, P. Maisonneuve, Natural history of acute pancreatitis: A long-term population-based study, Am. J. Gastroenterol. 104 (2009) 2797–2805. https://doi.org/10.1038/ajg.2009.405.

[9] E. Bieliuniene, J.B. Frøkjær, A. Pockevicius, J. Kemesiene, S. Lukosevicius, A. Basevicius, G. Barauskas, Z. Dambrauskas, A. Gulbinas, Magnetic Resonance Imaging as a Valid Noninvasive Tool for the Assessment of Pancreatic Fibrosis, Pancreas. 48 (2019) 85–93. https://doi.org/10.1097/MPA.0000000000001206.

[10] J.B. Frøkjær, S.S. Olesen, A.M. Drewes, Fibrosis, atrophy, and ductal pathology in chronic pancreatitis are associated with pancreatic function but independent of symptoms, Pancreas. 42 (2013) 1182–1187. https://doi.org/10.1097/MPA.0b013e31829628f4.

[11] M.F. Akisik, A.M. Aisen, K. Sandrasegaran, S.G. Jennings, C. Lin, S. Sherman, J.A. Lin, M. Rydberg, Assessment of Chronic Pancreatitis: Utility of Diffusion-weighted MR Imaging with Secretin Enhancement, Radiology. 250 (2009) 103–109. https://doi.org/10.1148/radiol.2493080160.

[12] A. Madzak, S.S. Olesen, I.S. Haldorsen, A.M. Drewes, J.B. Frøkjær, Secretin-stimulated

MRI characterization of pancreatic morphology and function in patients with chronic pancreatitis, Pancreatology. 17 (2017) 228–236. https://doi.org/10.1016/j.pan.2017.01.009.

[13] J.B. Frøkjær, F. Akisik, A. Farooq, B. Akpinar, A. Dasyam, A.M. Drewes, I.S. Haldorsen, G. Morana, J.P. Neoptolemos, S.S. Olesen, M.C. Petrone, A. Sheel, T. Shimosoegawa, D.C. Whitcomb, Guidelines for the Diagnostic Cross Sectional Imaging and Severity Scoring of Chronic Pancreatitis, Pancreatology. 18 (2018) 764–773. https://doi.org/10.1016/j.pan.2018.08.012.

[14] H. Fukushima, S. Itoh, A. Takada, Y. Mori, K. Suzuki, A. Sawaki, S. Iwano, H. Satake, T. Ota, M. Ikeda, T. Ishigaki, Diagnostic value of curved multiplanar reformatted images in multislice CT for the detection of resectable pancreatic ductal adenocarcinoma, Eur. Radiol. 16 (2006) 1709–1718. https://doi.org/10.1007/s00330-006-0166-9.

[15] M. Barral, P. Soyer, W. Ben Hassen, E. Gayat, M. Aout, M. Chiaradia, A. Rahmouni, A. Luciani, Diffusion-weighted MR imaging of the normal pancreas: Reproducibility and variations of apparent diffusion coefficient measurement at 1.5-and 3.0-Tesla, Diagn. Interv. Imaging. 94 (2013) 418–427. https://doi.org/10.1016/j.diii.2012.12.007.

[16] T. Tirkes, Z.K. Shah, N. Takahashi, J.R. Grajo, S.T. Chang, S.K. Venkatesh, D.L. Conwell, E.L. Fogel, W. Park, M. Topazian, D. Yadav, A.K. Dasyam, Reporting Standards for Chronic Pancreatitis by Using CT, MRI, and MR Cholangiopancreatography: The Consortium for the Study of Chronic Pancreatitis, Diabetes, and Pancreatic Cancer, Radiology. 290 (2019) 207–215. https://doi.org/10.1148/radiol.2018181353.

[17] A. Schreyer, M. Jung, J. Riemann, C. Niessen, B. Pregler, L. Grenacher, A. Hoffmeister,

German Society of Digestive and Metabolic Diseases (DGVS), S3 Guideline for Chronic Pancreatitis – Diagnosis, Classification and Therapy for the Radiologist, RöFo - Fortschritte Auf Dem Gebiet Der Röntgenstrahlen Und Der Bildgeb. Verfahren. 186 (2014) 1002–1008. https://doi.org/10.1055/s-0034-1385005.

[18] J. Keller, P. Layer, Diagnosis of pancreatic exocrine insufficiency in chronic pancreatitis 2 . Pancreatic Function Tests, Pancreapedia. (2015) 1–7. https://doi.org/10.3998/panc.2015.37.

[19] S. V. DeSouza, R.G. Singh, H.D. Yoon, R. Murphy, L.D. Plank, M.S. Petrov, Pancreas volume in health and disease: a systematic review and meta-analysis, Expert Rev. Gastroenterol. Hepatol. 12 (2018) 757–766. https://doi.org/10.1080/17474124.2018.1496015.

[20] E.W. Szczepaniak, K. Malliaras, M.D. Nelson, L.S. Szczepaniak, Measurement of Pancreatic Volume by Abdominal MRI: A Validation Study, PLoS One. 8 (2013) 1–6. https://doi.org/10.1371/journal.pone.0055991.

[21] J.P. Kipp, S.S. Olesen, E.B. Mark, L.C. Frederiksen, A.M. Drewes, J.B. Frøkjær, Normal pancreatic volume in adults is influenced by visceral fat, vertebral body width and age, Abdom. Radiol. 44 (2019) 958–966. https://doi.org/10.1007/s00261-018-1793-8.

[22] N. Nissan, Modifications of pancreatic diffusion MRI by tissue characteristics: what are we weighting for?, NMR Biomed. 30 (2017) 1–11. https://doi.org/10.1002/nbm.3728.

[23] M. V Apte, M. V Apte, P.S. Haber, P.S. Haber, S.J. Darby, S.J. Darby, S.C. Rodgers, S.C. Rodgers, G.W. McCaughan, G.W. McCaughan, M.A. Korsten, M.A. Korsten, R.C. Pirola, R.C. Pirola, J.S. Wilson, J.S. Wilson, Pancreatic stellate cells are activated by

proinflammatory cytokines: implications for pancreatic fibrogenesis., Gut. 44 (1999) 534–541. http://eutils.ncbi.nlm.nih.gov/entrez/eutils/elink.fcgi?dbfrom=pubmed&id=10075961&retmode=ref&cmd=prlinks%5Cnpapers3://publication/uuid/25F9E3F1-D02A-4B91-9907-F6E726ECDCE4.

[24] M.G. Bachem, Z. Zhou, S. Zhou, M. Siech, Role of stellate cells in pancreatic fibrogenesis associated with acute and chronic pancreatitis, J. Gastroenterol. Hepatol. 21 (2006) 92–96. https://doi.org/10.1111/j.1440-1746.2006.04592.x.

[25] A. Masamune, T. Watanabe, K. Kikuta, T. Shimosegawa, Roles of Pancreatic Stellate Cells in Pancreatic Inflammation and Fibrosis, Clin. Gastroenterol. Hepatol. 7 (2009) S48–S54. https://doi.org/10.1016/j.cgh.2009.07.038.

[26] C. Brock, L.M. Nielsen, D. Lelic, A.M. Drewes, Pathophysiology of chronic pancreatitis, World J. Gastroenterol. 19 (2013) 7231–7240. https://doi.org/10.3748/wjg.v19.i42.7231.

[27] H. Schrader, B.A. Menge, S. Schneider, O. Belyaev, A. Tannapfel, W. Uhl, W.E. Schmidt, J.J. Meier, Reduced Pancreatic Volume and β-Cell Area in Patients With Chronic Pancreatitis, Gastroenterology. 136 (2009) 513–522. https://doi.org/10.1053/j.gastro.2008.10.083.

[28] J.H. Yoon, J.M. Lee, K.B. Lee, S.-W. Kim, M.J. Kang, J.-Y. Jang, S. Kannengiesser, J.K. Han, B.I. Choi, Pancreatic Steatosis and Fibrosis : Quantitative Assessment, Radiology. 000 (2016) 1–11. https://doi.org/10.1148/radiol.2015142254.

[29] J.M. Lee, S. Kannengiesser, Pancreatic Steatosis and Fibrosis : Quantitative Assessment, Radiology. 000 (2016) 1–11.

[30] H.H. Hu, H. Kim, K.S. Nayak, M.I. Goran, Assessment of Hepatic and Pancreatic Fat Fractions in Humans, Obesity (Silver Spring). 18 (2010) 841–847. https://doi.org/10.1038/oby.2009.352.Comparison.

[31] J. Li, C. Tang, Noninvasive Quantification of Pancreatic Fat in Healthy Phantom Construction of Fat Emulsions, Pancreas J. 40 (2011) 295–299.

[32] J.B. Frøkjær, M.V. Lisitskaya, S.S. Olesen, A.M. Drewes, T. Engjom, I.S. Haldorsen, T.S. study group, Systematic quantitative approach for assessment of imaging features in chronic pancreatitis patients: A feasibility and validation study, Pancreatology. 19 (2019) S38. https://doi.org/10.1016/j.pan.2019.05.096.

[33] N. Siddiqui, C.L. Vendrami, A. Chatterjee, F.H. Miller, Advanced MR Imaging Techniques for Pancreas Imaging, Magn. Reson. Imaging Clin. N. Am. 26 (2018) 323–344. https://doi.org/10.1016/j.mric.2018.03.002.

[34] M. Wang, F. Gao, X. Wang, Y. Liu, R. Ji, L. Cang, Y. Shi, Magnetic resonance elastography and T 1 mapping for early diagnosis and classification of chronic pancreatitis, J. Magn. Reson. Imaging. 48 (2018) 837–845. https://doi.org/10.1002/jmri.26008.

[35] T. Tirkes, D. Yadav, D.L. Conwell, P.R. Territo, X. Zhao, S.K. Venkatesh, A. Kolipaka, L. Li, J.R. Pisegna, S.J. Pandol, W.G. Park, M. Topazian, J. Serrano, E.L. Fogel, Magnetic resonance imaging as a non-invasive method for the assessment of pancreatic fibrosis

(MINIMAP): a comprehensive study design from the consortium for the study of chronic pancreatitis, diabetes, and pancreatic cancer, Abdom. Radiol. (2019). https://doi.org/10.1007/s00261-019-02049-5.

[36] N. Fujita, A. Nishie, Y. Asayama, K. Ishigami, N. Fujimori, T. Ito, H. Honda, Intravoxel incoherent motion magnetic resonance imaging for assessment of chronic pancreatitis with special focus on its early stage, Acta Radiol. (2019) 028418511987268. https://doi.org/10.1177/0284185119872687.

[37] A. Parakh, T. Tirkes, Advanced imaging techniques for chronic pancreatitis, Springer US, 2019. https://doi.org/10.1007/s00261-019-02191-0.

[38] T. Tirkes, C. Lin, E. Cui, Y. Deng, P.R. Territo, K. Sandrasegaran, F. Akisik, Quantitative MR evaluation of chronic pancreatitis: Extracellular volume fraction and MR relaxometry, Am. J. Roentgenol. 210 (2018) 533–542. https://doi.org/10.2214/AJR.17.18606.

Figure legends:

Fig. 1: Study flowchart of patient enrolment.

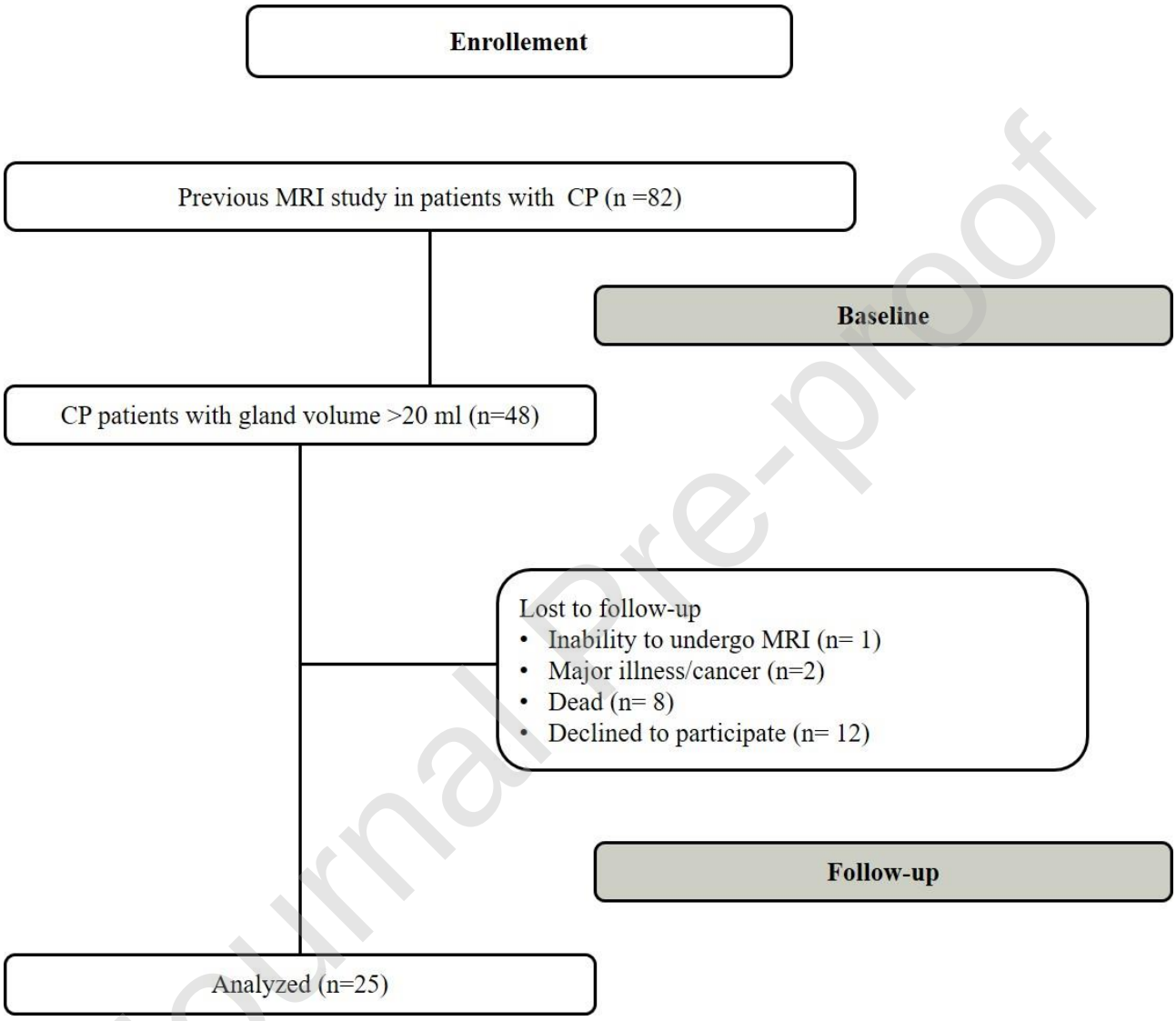

Fig. 2: Magnetic resonance imaging of a representative patient with chronic pancreatitis at the baseline scanning and 4-year follow-up. All images were acquired using the same 1.5 Tesla scanner. Assessment of anterior-posterior diameter (A) in the pancreatic body on T2-weighted images. Apparent diffusion coefficient maps (DWI) with a ROI positioned in the pancreatic head (B) for

assessment of parenchymal fibrosis (reduced apparent diffusion coefficients values represent restricted diffusion). Assessment of pancreatic fat content on two-point Dixon imaging with fat-only (C) and water-only (D), with region of interest positioned in the pancreatic head and body. 3-dimensional magnetic resonance cholangiopancreatography (E) showing dilated and irregular MPD and abnormal side branches (arrows). Abbreviations: MPD, main pancreatic duct; CBD, common bile duct; GB, gallbladder.

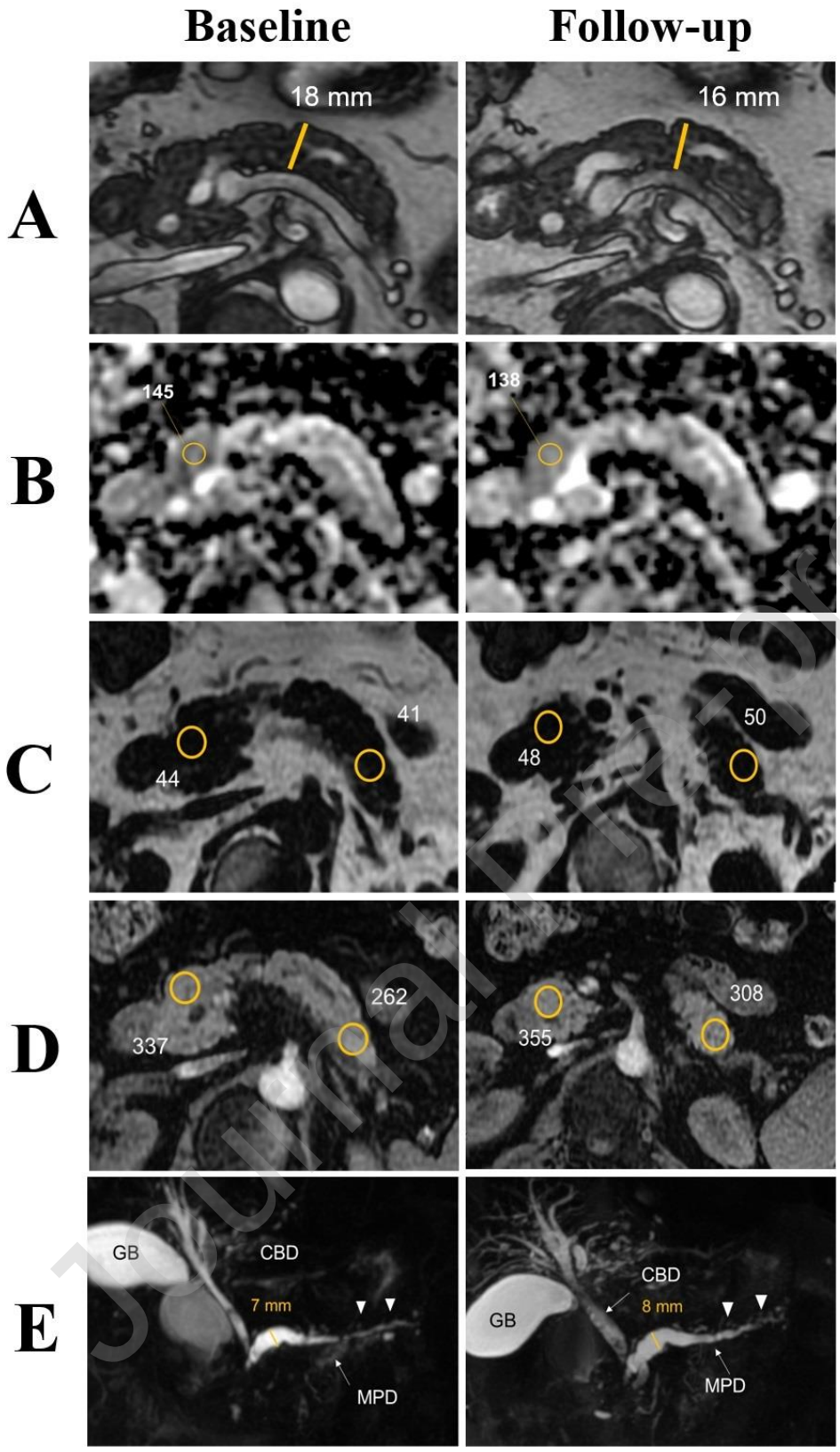

Fig. 3: Box-plots showing the progression of morphological imaging parameters in chronic pancreatitis between initial baseline scanning and four-year follow-up. A: Pancreatic gland volume. B: Degree of water diffusion (expressed as apparent diffusion coefficient) in the head, body, and tail of the pancreas. C: Pancreatic fat content (expressed as fat signal fraction) in the pancreatic head, body and tail. D: Anterior-posterior diameter of the main pancreatic duct in the head, body and tail.

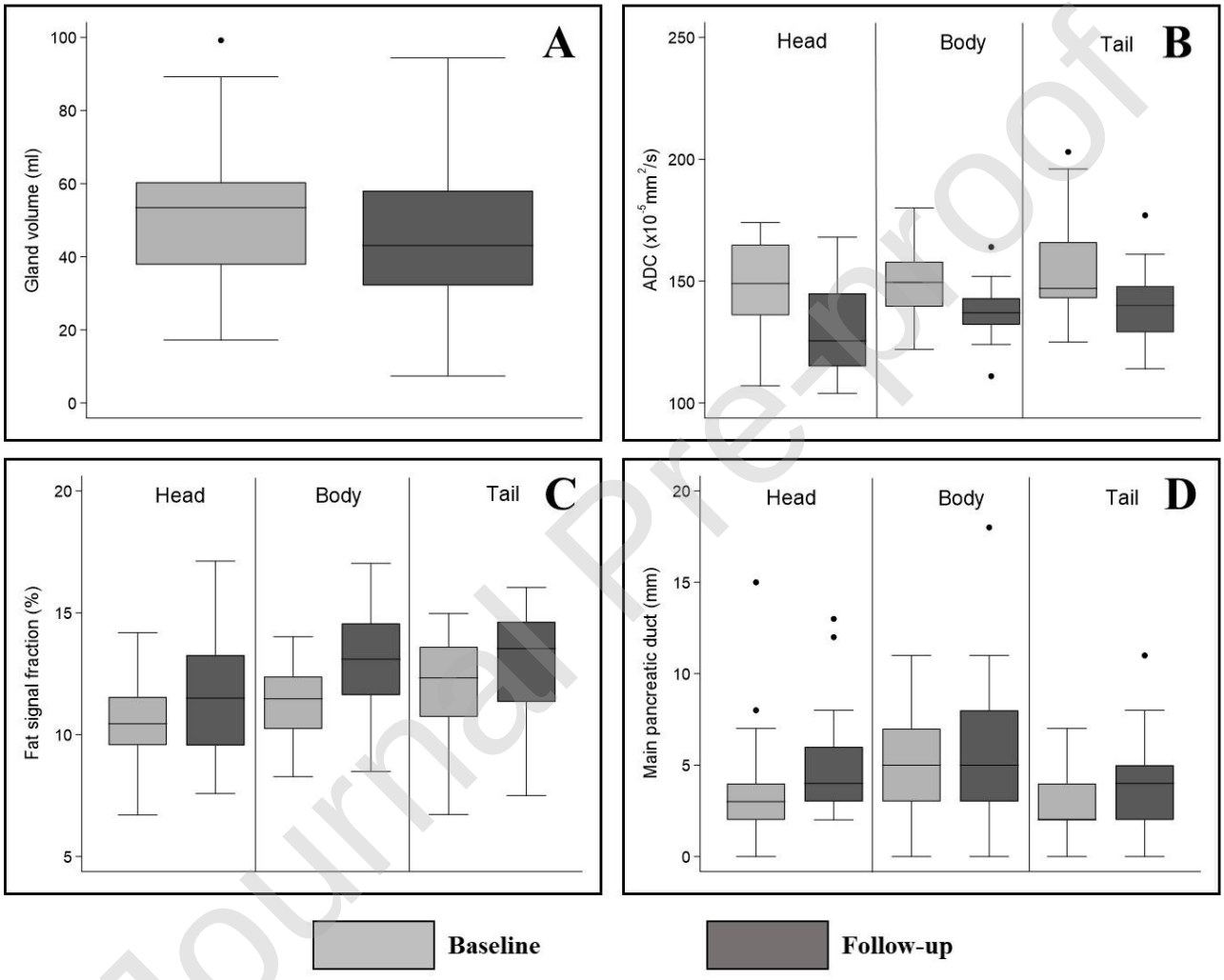

Table 1:

Baseline demographic and clinical characteristics of the patients

	Baseline (n=25)
Age, mean (SD), years	60.3 (8.5)
Sex, n (%)	
• Male	13 (52)
• Female	12 (48)
Duration of CP, mean (range), years	7.8 (2-22)
BMI, mean (SD), kg/m2	24.1 (3.3)
Aetiology, n (%)	
• Toxic-metabolic	11 (44)
• Other	14 (56)
Diabetes mellitus, n (%)	4 (16)
Exocrine insufficiency, n (%)	12 (48)

Note: Descriptive statistical values are represented as percentages (%), mean (SD) or mean (range).

Abbreviations: MRI, magnetic resonance imaging; CP, chronic pancreatitis; BMI, body mass index.

Table 2:

Morphologic characteristics of CP patients at baseline and at 4-year follow-up

	Baseline (n= 25)	**Follow-up (n=25)**	**P**
Gland volume in ml, mean (SD)	50.3 (19.6)	43.5 (20.8)	<0.001
Gland AP diameter in mm, mean (SD)			
• Head	25.4 (6.7)	23.7 (6.9)	<0.001
• Body	15.4 (4.2)	13.3 (4.6)	<0.001
• Tail	15.3 (4.1)	13.3 (4)	<0.001
ADC (x10^{-5}mm²/s), mean (SD)			
• Head	145.9 (17.1)	130.1 (14.2)	<0.001
• Body	147.3 (13.7)	136.7 (11.1)	<0.001
• Tail	150.8 (17.9)	136.8 (15.6)	0.002
FSF in %, mean (SD)			
• Head	10.6 (1.8)	11.4 (2.3)	<0.001
• Body	11.3 (1.2)	12.8 (2.5)	<0.001
• Tail	12.8 (5.1)	14.1 (6.6)	0.024
Irregular contour, n (%)	6 (24)	8 (32)	0.317
Irregular structure, n (%)	4 (16)	3 (12)	0.317
Continuous organ involvement, n (%)	7 (28)	8 (32)	0.317
Pseudocysts with diameter > 5 mm, n (%)	8 (32)	9 (36)	0.739
Maximal overall MPD in mm, mean (SD)	5.5 (3)	6.7 (3.9)	0.230
• MPD diameter (head)	3.8 (3)	4.8 (3)	0.131
• MPD diameter (body)	4.8 (2.5)	5.7 (3.7)	0.421
• MPD diameter (tail)	3.2 (1.8)	3.8 (2.5)	0.737
Dilated side-ducts, n (%)	21 (84)	22 (88)	0.317
Ductal obstruction, n (%)	5 (20)	5 (20)	1.000
Intraductal calculus, n (%)	2 (8)	3 (12)	0.317
Intraductal filling defects, n (%)	2 (8)	4 (16)	0.317
Modified Cambridge classification score			0.033
• 0 - Normal	1 (4)	1(4)	
• 1 - Equivocal	2 (8)	1(4)	
• 2 - Mild CP	6 (24)	4 (16)	
• 3 - Moderate CP	10 (40)	7 (28)	
	6 (24)	12 (48)	

- 4 - Marked CP

Note: Descriptive statistical values are represented as percentages (%) or mean (SD). Abbreviations: CP, chronic pancreatitis; AP, anterior-posterior; ADC, apparent diffusion coefficient; FSF, fat signal fraction; MPD, main pancreatic duct

Table 3 :

Correlation analyses between morphological MRI parameters in patients with CP at the baseline

HEAD						
	1	2	3	4	5	6
1.Maximal MPD diameter head, mm	1					
2.Cambridge classification	0.28	1				
3.Gland volume, ml	-0.17	-0.34	1			
4.AP diameter head, mm	0.07	0.02	**0.7*** **	1		
5.ADC head, $x10^{-5}mm^2/s$	0.03	**0.49***	-0.33	-0.31	1	
6.FSF head, %	0.12	0.18	0.11	0.06	0.08	1

BODY						
	1	2	3	4	5	6
1.Maximal MPD diameter body, mm	1					
2.Cambridge classification	**0.52****	1				
3.Gland volume, ml	-0.24	-0.34	1			
4.AP diameter body, mm	-0.10	-0.05	**0.46****	1		
5.ADC body, $x10^{-5}mm^2/s$	0.00	0.15	-0.27	-0.33	1	
6.FSF body, %	0.44	0.37	-0.11	-0.01	-0.25	1

TAIL						
	1	2	3	4	5	6
1.Maximal MPD diameter tail, mm	1					
2.Cambridge classification	0.37	1				
3.Gland volume, ml	-0.10	-0.34	1			
4.AP diameter tail, mm	-0.42	0.11	**0.43***	1		
5.ADC tail, $x10^{-5}mm^2/s$	0.36	0.07	-0.25	0.07	1	
6.FSF tail, %	0.02	0.14	-0.24	0.05	-0.31	1

Note: *P-value < 0.05, **P-value < 0.01, ***P-value < 0.001. Numbers 1- 6 under Correlations correspond to the MRI parameters numbered 1-6. All correlations analyses were performed using Pearson correlation except for correlations with Cambridge classification scores were Spearman's correlation test were used. Significant correlation coefficients are given in bold. Correlations between main pancreatic duct and Cambridge classification were not performed as these parameters are not mutually independent.

Abbreviations: MRI, magnetic resonance imaging; CP, chronic pancreatitis; MPD, main pancreatic duct; AP, anterior-posterior; ADC, apparent diffusions coefficient; FSF, fat signal fraction.

Table 4 :

Correlation analyses between progression of morphological MRI parameters in patients with CP

HEAD						
	1	2	3	4	5	6
1.ΔMaximal MPD diameter head, mm	1					
2.ΔCambridge classification	0.33	1				
3.ΔGland volume, ml	0.29	0.2	1			
4.ΔAP diameter head, mm	0.39	0.06	**0.7*** **	1		
5.ΔADC head, x10^{-5}mm²/s	-0.07	0.07	-0.07	-0.19	1	
6.ΔFSF head, %	0.27	**0.49***	-0.16	-0.02	0.09	1

BODY						
	1	2	3	4	5	6
1.ΔMaximal MPD diameter body, mm	1					
2.ΔCambridge classification	0.36	1				
3.ΔGland volume, ml	0.22	0.22	1			
4.ΔAP diameter body, mm	0.26	0	**0.64*** **	1		
5.ΔADC body, x10^{-5}mm²/s	0.14	-0.02	0.07	-0.09	1	
6.ΔFSF body, %	-0.15	-0.35	0.03	-0.27	-0.23	1

TAIL						
	1	2	3	4	5	6
1.ΔMaximal MPD diameter tail, mm	1					
2.ΔCambridge classification	**0.67*** **	1				
3.ΔGland volume, ml	0.16	0.22	1			
4.ΔAP diameter tail, mm	-0.15	0	**0.55****	1		
5.ΔADC tail, x10^{-5}mm²/s	-0.39	**-0.61****	0.26	0.25	1	
6.ΔFSF tail, %	0.39	0.14	0.22	0.15	-0.03	1

Note: *P-value < 0.05, **P-value < 0.01, ***P-value < 0.001. Δ indicates change between baseline and follow-up. Numbers 1- 6 under Correlations correspond to the MRI parameters numbered 1-6. All

correlations analyses were performed using Pearson correlation except for correlations with Cambridge classification scores were Spearman's correlation test were used. Significant correlation coefficients are given in bold. Correlations between main pancreatic duct and Cambridge classification were not performed as these parameters are not mutually independent. Abbreviations: MRI, magnetic resonance imaging; CP, chronic pancreatitis; MPD, main pancreatic duct; AP, anterior-posterior; ADC, apparent diffusions coefficient; FSF, fat signal fraction.